Aromatic Ionomer Membranes. I. Physical and Mechanical Properties

E. BESSO, R. LEGRAS, and A. EISENBERG, *Department of Chemistry, McGill University, Montreal, Quebec, H3A 2K6, Canada,* R. GUPTA, *Daychem Laboratories, Dayton, Ohio,* F. W. HARRIS, *Institute of Polymer Science, University of Akron, Akron, Ohio,* and A. E. STECK and H. L. YEAGER, *Department of Chemistry, University of Calgary, Calgary, Alberta, T2N 1N4, Canada*

Synopsis

The physical properties of a new class of ionomers comprising a semirigid polyphenylene ether backbone were investigated. The material was studied principally in the form of films of ca. 150 μm micrometers in thickness. The study focused on material of 600 equivalent weight. Torsion pendulum results showed a significant increase in the glass transition temperature of the ionomer relative to that of its ester precursor but gave no evidence of ionic clustering. Stress–strain studies performed both in water and in 20% KOH solution at 80°C indicated that the mechanical properties of the material remain stable under these conditions. Differential scanning calorimetry was used to investigate both the high temperature behavior and the water uptake of the ionomer films. The behavior of this ionomer at high temperature and in an alkaline solution is of particular interest in view of the possible use of these films as separators in an alkaline electrolysis cell.

INTRODUCTION

Ionomers have developed, in the past 20 years, into a distinct and promising branch of the polymer field. These systems of relatively low ion content are partly hydrophilic but generally insoluble in water. Their structure and mechanical properties differ significantly from those of their nonionic parent polymers. In the systems studied to date, ion incorporation has been found to raise the glass transition temperature dramatically and, in some cases, to introduce complex thermorheological behavior. The properties of several ionomer systems have been described in the literature,[1,2] in particular those based on ethylene,[3–10] styrene,[11–17] and tetrafluoroethylene (Nafions).[18]

Ion aggregation, effected through dipole–dipole interaction of the pendant ion pairs, constitutes the structural basis which underlies the properties characteristic of most ionomers studied to date. At appreciable ion concentrations, their structure can broadly be described as that of a microphase-separated system in which a matrix of low ionic content is interspersed with ion-rich domains.

Aromatic ionomers constitute a new class of high glass transition systems. They originated with the recent synthesis of carboxylated-phenylated polyphenylenes.[19–21] A preliminary investigation of the dynamic-mechanical

Journal of Applied Polymer Science, Vol. 30, 2821–2836 (1985)
© 1985 John Wiley & Sons, Inc. CCC 0021-8995/85/072821-16$04.00

and stress–relaxation behavior of two potassium salts[22] is the only reported study of the mechanical properties of these systems to date. The aim of the present study was to explore further the structure and mechanical properties of these novel materials, particularly in the form of thin films. Their good thermal and chemical stability render them particularly interesting for applications in aggressive environments such as concentrated potassium hydroxide solution at 180°C. This aspect will be discussed in a subsequent paper.

The structural formulae of the nonionic ester precursor and of the ionomer are shown in Figure 1. The molar ratio of *X* to *Y* determines the attainable ionic content of the material. The equivalent weights and corresponding ionic contents for various molar ratios are shown in Table I. In the subsequent text, mention of equivalent weight alone (e.g., 600EW) will be used to designate the ionomer (potassium salt) obtained by alkaline hydrolysis of the ester. The precursor will be denoted by the equivalent weight followed by "ester" (e.g., 600EW ester). The material used in the studies discussed below is of equivalent weight 600 unless specified otherwise.

By choosing different film preparation methods, a wide variety of structures can be obtained. These range from a dense cohesive material showing a typical water uptake of ca. 15% to extremely porous material showing water absorptions of up to 700%. The latter films are made by methods similar to those developed in the cellulose acetate technology.[23] This publication will focus on the ionomeric material of intermediate porosity obtained by hydrolysis of the ester precursor already in film form. It has proved to be the most interesting to date in view of its possible use as a separator for electrolytic cells operating under alkaline conditions.

EXPERIMENTAL

Sample Preparation. The ionomer films were prepared by one of the following methods. The first route entailed a hydrolysis of the ester, in powder form, to the salt also in powder form. The ionomer was subsequently dissolved in DMSO, hot filtered, and then cast on a glass plate at a high temperature. Solvent evaporation yielded a dense, cohesive film which was further dried under reduced pressure until constant weight was achieved. The product of this method will be designated by the equivalent weight followed by the suffix p (e.g., 600EW-p).

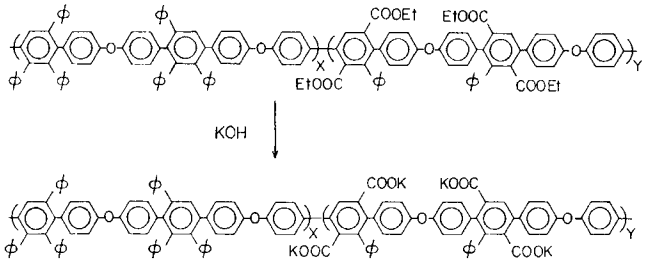

Fig. 1. General structure of aromatic polyphenylene ether in the nonionic (ester) precursor and potassium ionomer (salt) form.

TABLE I
Nomenclature and Ionic Content of Aromatic Ionomers

Designation	X	Y	% Ionic groups/ pendant phenyl groups
1200EW	0.8	0.2	10
800EW	0.7	0.3	15
600EW	0.6	0.4	20
400EW	0.4	0.6	30

The second method entailed the manufacture of a precursor film of the desired dimensions. This was done by casting a solution of the precursor onto a glass plate and allowing the solvent to evaporate at room temperature. The resultant film was then hydrolyzed at high temperature and pressure. By varying hydrolysis conditions such as temperature, pressure or concentration, a wide range of results can be obtained. These films shall be designated by the 600EW-f nomenclature.

Characterization. Viscosity of the ester materials in chloroform was measured in an Ubbelohde viscometer at 30°C. Density of the 600EW ester was determined by the hydrostatic weighting method.[24] Thermogravimetric analyses (TGA) were performed using a quartz spring apparatus at heating rates of ca. 5°C/min. Thermal stability experiments were run under reduced pressure (ca. 3 mm Hg) whereas water content experiments were run in air. Infrared data were obtained on a Nicolet 7199 FTIR instrument.

Calorimetry. The Perkin-Elmer DSC-2 differential scanning calorimeter was used to determine the heats of fusion of water associated with the samples. Wet films (ca. 5–10 mg) were placed in stainless steel pans specially designed for volatile samples. These were hermetically sealed, placed in the sample holder, and quenched to −73°C. After 10 min at that temperature, scanning was conducted at a rate of 10°C/min.

The total water content in each pan was determined by weighing. To obtain the dry weight, the cap was punctured, and the pan set to dry overnight at 150°C under reduced pressure.

Glass transition temperatures were determined at a scan rate of 20°C/min on thick film samples.

Stress–Strain Behavior. Stress–strain measurements in the tensile mode were performed on an Instron tester (Model 1122) modified by the addition of a chamber allowing testing under water or in a solution. The experiments were performed at 25°C in air and at 80°C in water, in dilute (0.1*M*) and in concentrated (20%) KOH solution. Film samples of ca. 130 μm in thickness were allowed to reach equilibrium prior to testing. A constant elongation rate of 2 mm/min was used in all cases. The results obtained are an average of 2–5 runs.

Microscopy and X-Ray Diffraction. Electron micrographs were obtained on an ISI model SX-30 Scanning Electron Microscope (SEM) operating at 15 kV. The wide angle X-ray diffraction (WAXD) patterns were obtained on a Phillips PW 1730 X-ray generator with CuKα incident radiation at 40 kV and 35 mA. The photographs were analyzed with a Joyce microdensitometer.

Dynamic Mechanical and Stress Relaxation Behavior. Dynamic mechanical behavior was studied using a free vibration torsion pendulum[25] operating at ca. 1 Hz and a vibrating reed spectrometer[26,27] at higher frequencies. Heating rates were always below 1°C/min. For these experiments only, samples were compression-molded at 290°C for 15 min at a load of 14 MPa.

Stress–relaxation experiments were performed under water on an instrument described in an earlier publication.[28] The stress at constant strain was measured for a series of temperatures ranging from 25 to 80°C. Thin film samples were allowed to reach their equilibrium water uptake (ca. 20 h) prior to each experiment. A comprehensive general discussion of stress–relaxation and dynamic mechanical behavior may be found in the literature.[29,30]

RESULTS

Both methods of film preparation yield films which show great affinity for water. The water uptake, as well as the size and distribution of pores, are strongly dependent on the method of preparation. The water retained falls into a minimum of two categories. A preliminary DSC investigation into the nature of the bonding between water and polymer at low temperature[31] will be discussed.

General Characterization. The intrinsic viscosity for 600EW ester precursor in chloroform at 30°C ranged from 0.75 to 1.055 dL/g. The 600EW ester was found to have a density of 1.38 $\pm$ 2% g/cc. Conversion of the ester precursor to the ionomer was verified by FTIR through the measurement of the intensity of the carbonyl salt stretching vibration at ca. 1575 cm^{-1}. Taken as a ratio of the weaker ether CO stretching vibration occurring at 1171 cm^{-1}, a minimum value of 1.25 for I_{1575}/I_{1171} was taken to signify complete (>95%) conversion. IR absorption at the ester carbonyl vibration frequency of 1730 cm^{-1} did not disappear in all cases and will be discussed further. TGA shows the beginning of weight loss at ca. 375°C for 600EW ester, the total loss closely corresponding to the calculated weight percentage of ethoxycarbonyl groups present in the material.

The high temperature DSC studies showed a large endotherm peaking at ca. 400°C for the esters; it was absent in the ionomers. Typical curves are shown for the 600EW materials in Figure 2. In the ester precursors, the heats corresponding to this high temperature peak increase with increasing ethoxycarbonyl content. This endotherm is due to the decarboxylation reaction and marks the onset of sample degradation.

Glass Transition. Glass transition temperatures were determined by two independent methods on the dry polymers. In the torsion pendulum runs, the peak of the tan δ vs. temperature curve was taken as the T_g. Figure 3 shows the curves obtained for 800EW ester and 800EW-p. A molded sample of 600EW-p could not be obtained since the material begins to decompose at molding temperatures.

In DSC, the ester precursors display almost identical glass transition temperatures at ca. 290°C. The ionomers show a transition at higher temperature, in addition to one at ca. 290°C (Fig. 2). This high temperature

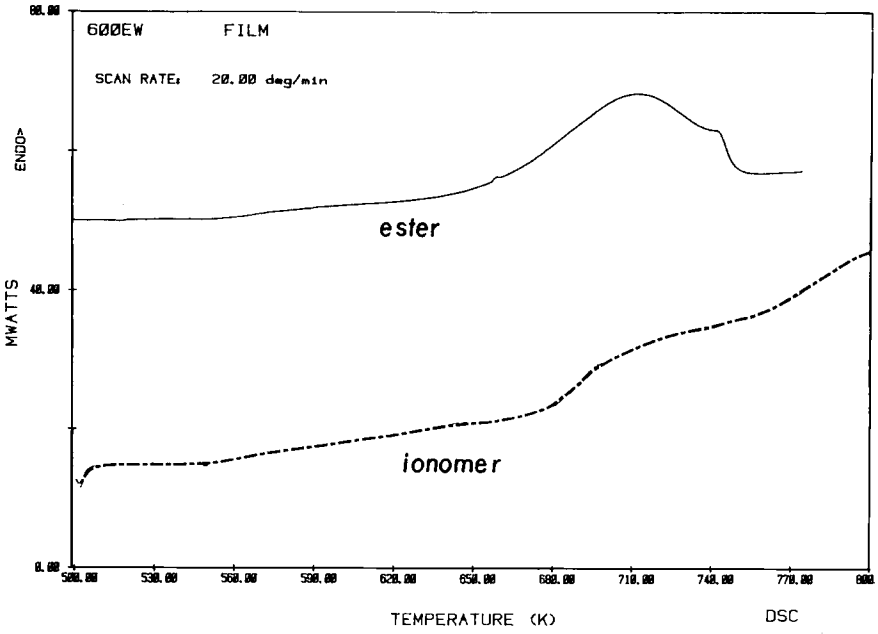

Fig. 2. Differential scanning calorimetry curves for 600EW precursor and ionomer.

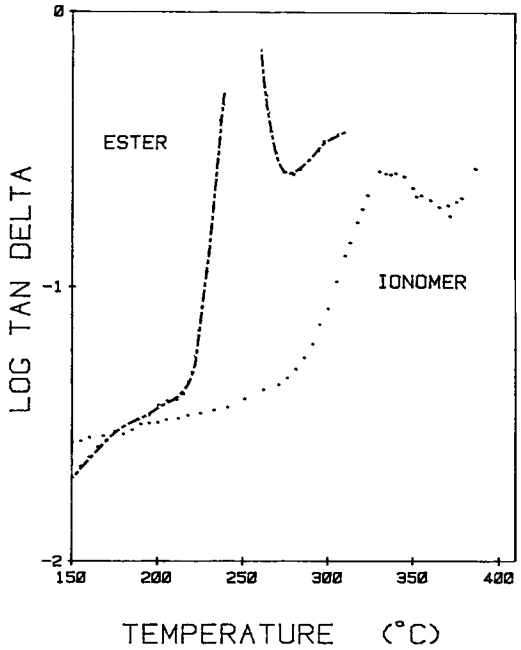

Fig. 3. Mechanical loss tangent as a function of temperature for 800EW precursor and ionomer.

transition moves to higher temperature with increasing ionic content and may be related to ionic aggregates. The results obtained are shown in Table II. The transition temperatures obtained by torsion pendulum and DSC are not identical; however, differences of ca. 40 degrees appear to be quite consistent.

Mechanical Properties. Dynamic mechanical testing of the esters of 400, 600, and 800 equivalent weight at low frequency (ca. 2 Hz) indicates, in addition to the glass transition, a single broad peak in the loss tangent at low temperature (ca. −100°C). In the ionomer, a similar low temperature peak is observed, but the glass transition shifts to higher temperature (Fig. 3). The loss tangent curves obtained at higher frequency from vibrating reed experiments for the same materials show corresponding low temperature dispersions at slightly higher temperatures. An Arrhenius-type plot for the 800EW ionomer indicates an activation energy of ca. 13 kcal/mol for this low-temperature dispersion, a value in agreement with that previously found for the 1200EW material.[22]

Dry stress–strain tensile testing of the 600EW ester film at 25°C repeatedly shows a definite yield point and large strains at break (> 150%). These were the first indications of the presence of orientation in the system. Results obtained under water and in dilute KOH solution do not differ significantly. The results obtained under water and in 20% KOH solution are given in Table III for the aromatic systems as well as for Nafion. Sample history was found to influence behavior of the sample under tensile stress. Figure 4 shows the stress–strain curves for three 600EW-f samples that underwent various pretreatments. Although the modulus of the sample dried under vacuum at 115°C for 5 days (a) is only slightly higher than those of the two other samples, a large difference in energy to break, or toughness, is evident. The sample dried under the more strenuous conditions can absorb only one half the energy necessary to break the other two samples.

Orientation. The presence of orientation was investigated further by WAXD of the strained and unstrained 600EW ester and 600EW-f. Microdensitometer traces of the resultant exposures are shown in Figure 5 and clearly indicate a low degree of orientation that is enhanced in the strained ester sample.

Contact Angle, SEM, and Water Uptake. Measurements of the contact angle of water on freshly prepared thin film surfaces as a function of time show a decrease of ca. 70° for 600EW-f over a period of 3 min. A parallel study on Nafion 1200 shows a decrease of only 10° over the same time

TABLE II
Transition Temperatures (°C) for the Dry Polymers

	Torsion pendulum		D S C	
Sample	Precursor	Ionomer	Precursor	Ionomer
1200EW[23]	257	280	—	355
800EW	250	330	292	405
600EW	255	—	290	420
400EW	243	—	285	440

TABLE III
Stress–Strain Results at 80°C under Water (W) and in 20% KOH

	Modulus (MPa)		Tensile strength (MPa)		Energy to break (J)		Break strain (%)	
	W	KOH	W	KOH	W	KOH	W	KOH
600EW ester	1500	1500	40	50	0.60	1.3	80	85
600EW-f	200	200	20	20	0.2	0.2	30	30
Nafion 1200	60	120	20	17	1.3	0.5	400	200

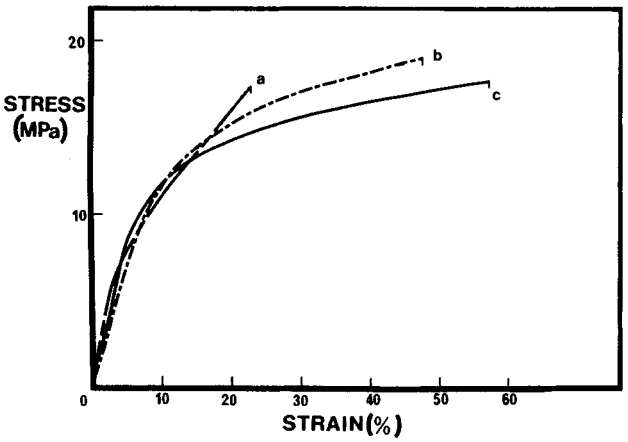

Fig. 4. Stress–strain curves, in 20% potassium hydroxide at 80°C, showing the effect of drying: (a) dried at 100°C under reduced pressure; (b) dried at STP; (c) continuously kept in water. (—) never dried; (- - — - — -) dried, ambient; (— - -) dried, 100°C, vac.

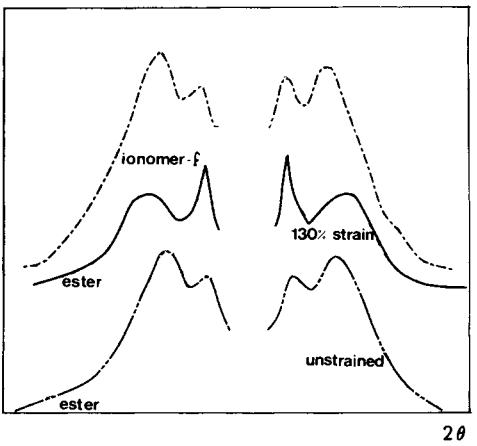

Fig. 5. Microdensitometer traces of wide angle X-ray diffraction patterns for strained and unstrained 600EW ester and for 600EW-f.

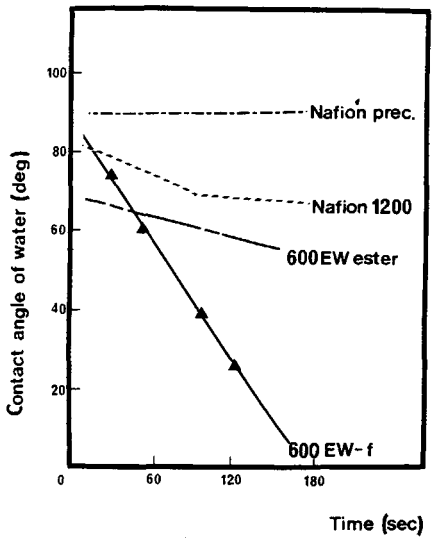

Fig. 6. Contact angle of water as a function of time for 600EW materials and Nafion 1200.

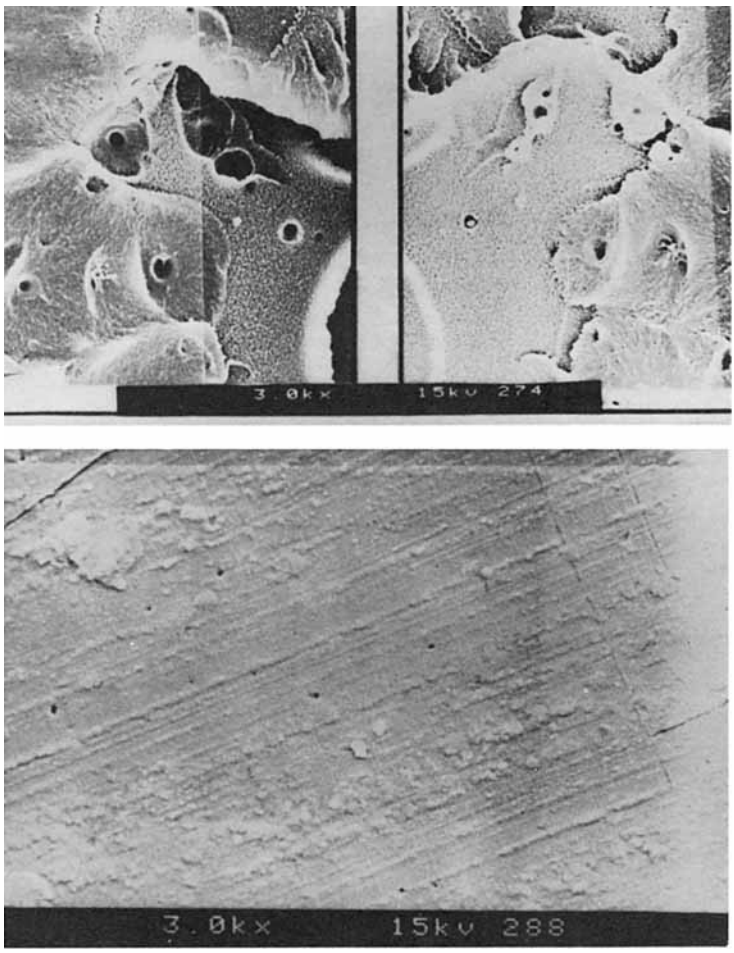

Fig. 7. Scanning electron micrographs of 600EW ionomer: (a) cut surface; (b) film surface.

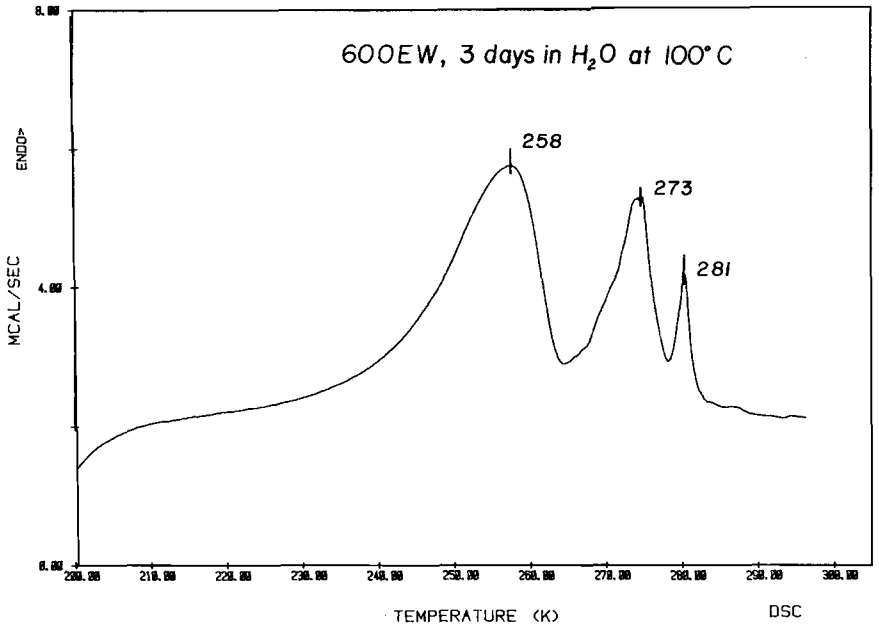

Fig. 8. Differential scanning calorimetry curve for 600EW ionomer film kept in water at 100°C for 3 days.

interval. These results are shown in Figure 6 for the 600EW materials and for Nafion.

Surfaces and cuts of 600EW ester and 600EW-f were studied by SEM (Fig. 7). Holes of diameters ranging from 0.5 to 100 μm are evident throughout the ionomer cut surface. The surface of the sample also shows pinholes of diameters ranging from 0.5 to 5 μm.

Micrographs of the ester show similar features, with comparable pore dimensions in both surface and fracture. However, the ester cut surface shows fewer pores. The higher void content of the ionomer film may be due to the process of hydrolysis by which the ester is transformed to the ionomer.

DSC measurements at subambient temperature of 600EW-f ionomer films kept in water at ambient temperature[31] give the result shown in Figure 8. After 1 day in water, 600EW-f exhibits a triple endotherm corresponding to the fusion of the water absorbed. The small peak at the highest temperature is due to residual (or free) water remaining after incomplete wiping. The fact that it appears at a temperature higher than 273°K is explained by the time lag experienced in the heating of material (surface water) which is not in direct contact with the heating block. The two endotherms which appear at lower temperature reflect the fusion of the water held within the material. The fact that a double melting peak occurs for the same process suggests two distributions in the size of pores in the sample. The first distribution peaks at 0°C and corresponds to the large size porosity observed by SEM. The second one may correspond to a microporosity not visible by SEM. If this freezing point depression of 20°C is indeed due to porosity of very small dimension, then it can only correspond to a capillary diameter below 1000 Å,[32] which is near the resolution limit of SEM.

The approximate water content corresponding to each endotherm was calculated by assuming the enthalpy of fusion for water held in capillaries to be identical to that of pure water. Although the assumption of a heat of fusion of 80 cal/g is admittedly incorrect in this circumstance, it was used nonetheless to obtain a rough estimate of the proportion of water residing in these different environments. For 600EW-f, these two areas yield a total aqueous content of 50%. Since the total water uptake measured by weight was ca. 80% (±10%), roughly 30% of the water appears to be ion-bound. For 600EW-p, the equilibrium water uptake reaches only 15% (by weight measurement), and no freezing water endotherm can be observed by DSC. It should be stressed again that these numbers are highly approximate. It has been found, moreover, that the time of residence in water, the temperature of the water, and other preliminary treatments (subjection to high temperature, vacuum, etc.) influence the water uptake of 600EW-f as well as the detailed shape of the DSC curve. Hydrolysis conditions were also found to affect the water uptake.

By TGA, a rapid decrease of the weight of the water-containing samples is observed at low temperature. The slope of the TGA curve decreases at ca. 100°C, indicating a slower weight loss. Above 200°C, no significant change in weight is observed until the degradation process occurs.

A total water uptake of 100% is recorded for a sample which had been kept in water at ambient temperature for 2 months. It is proposed that the rapid weight loss is due to removal of the free water observed in DSC while the ion-bound water must disappear at higher temperature.

Stress–Relaxation. Results of underwater stress relaxation experiments for 1200EW-p, 600EW-f,[33] and Nafion 1200[28] are shown in Figure 9 as isochronal modulus–temperature plots. The modulus of Nafion appears lower

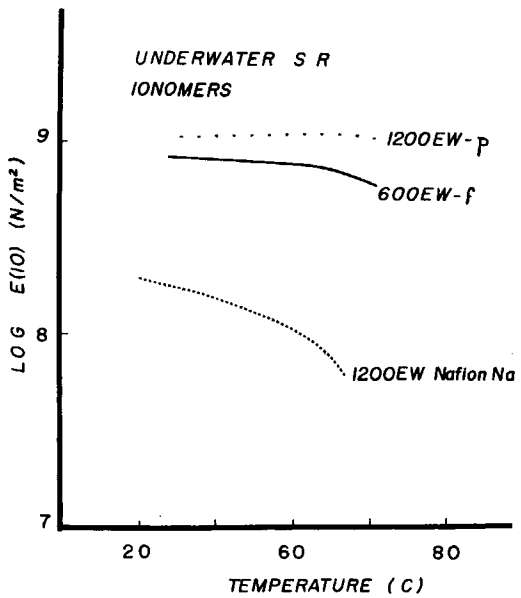

Fig. 9. Underwater stress relaxation curves for 1200EW and 600EW aromatic carboxylate ionomers and for Nafion 200.

than that of the aromatic ionomers. This is explained by the fact that, in addition to the plasticizing effect of ca. 10% water absorption, Nafion is much closer to its glass transition temperature than either of the other two systems. The aromatic 1200EW-p is seen to absorb much less water than 600EW-f, this being the reason for the lower modulus of the latter.

DISCUSSION

As indicated by the values of intrinsic viscosity, the 600EW ester studied is of high molecular weight. There is no evidence that any degradation occurs during hydrolysis to obtain the ionomer under the conditions used. Comparison of electron micrographs shows only a slight increase in void content in the ionomer fracture relative to that of the ester precursor. Progressive lengthening of the reaction time at the same temperature and pressure yielded increasingly brittle material.

Crosslinking

Comparison of the FTIR spectra of several films hydrolyzed under differing conditions showed variations in the intensity of the ester carbonyl band at ca. 1730 cm^{-1}. Theoretically, this band should disappear in the completely hydrolyzed ionomer. It is indeed absent in the FTIR spectra of samples hydrolyzed at lower pressure [Fig. 10(a)]. However, under some experimental conditions, this band reaches a minimum absorbance intensity but does not completely disappear [Fig. 10(b),(c)]. The intensity of the asymmetric carbonyl absorbance of the salt (at ca. 1575 cm^{-1}) was comparable in all cases.

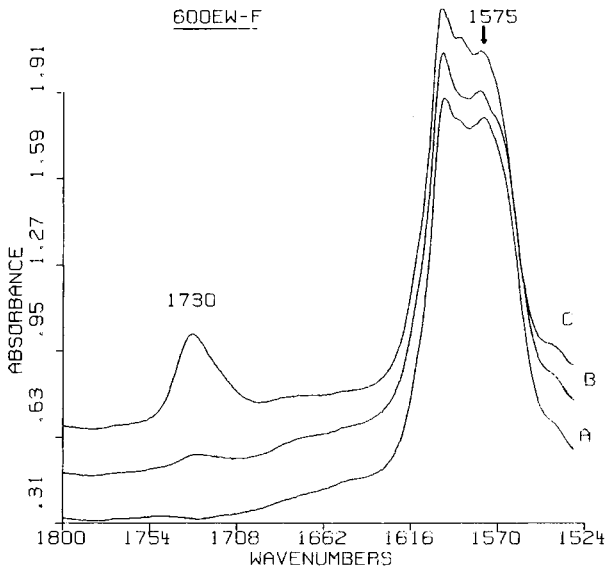

Fig. 10. Infrared spectra of 600EW ionomer samples showing different carbonyl absorbance intensities at a frequency of 1575 wavenumber.

This observation suggests the occurrence of crosslinking in the polymer when hydrolysis takes place under high pressure. Two of the possible mechanisms are the formation of an anhydride crosslink and the formation of an ester crosslink. The first possibility can be readily dismissed because the IR spectra show no evidence of the two bands expected from the vibrational coupling of anhydride carbonyl groups.[34] The second possibility, the ester crosslink, is thought to develop via a base-catalyzed transesterification reaction between the polymer and ethylene glycol. This is schematically shown below.

$$R\text{-}CO_2C_2H_5 \underset{KOH}{\overset{C_2H_4(OH)_2\,/\,H_2O}{\rightleftharpoons}} R\text{-}CO_2C_2H_4OH + C_2H_5OH \quad (1)$$

$$2\ R\text{-}CO_2C_2H_4OH \rightleftharpoons R\text{-}CO_2\text{-}C_2H_4\text{-}O_2C\text{-}R \quad (2)$$

where R = polymer chain. In eq. (2), the recombinant species need not be identical but could also involve an acid or ester moiety. Whether or not this crosslink truly occurs is not known, especially in view of the low concentration of ionic units and also of ethylene glycol in the sample. Nevertheless, whatever reaction occurs appears to affect the product significantly.

The crosslinking hypothesis was further verified by stress–strain testing in 0.1*M* KOH of samples whose FTIR spectra show varying degrees of relative absorbance at 1730 cm^{-1} but comparable relative absorbance at 1575 cm^{-1}. As expected if crosslinking had occurred, the ionomer sample with a higher residual ester CO absorbance band showed a correspondingly higher modulus than the others (Fig. 11).

Torsion Pendulum

Torsions pendulum results for the 1200EW and 800EW materials showed a marked effect on the glass transition temperature with ion incorporation. An increase of 2–5°/mol % pendant ionic groups was observed and is consistent with other ionomer systems studied to date.[2]

The glass transition temperatures of the ester precursors determined by DSC show a difference of ca. 40° (Table II) relative to those obtained by torsion pendulum. A similar difference in glass transition temperature has been reported for some phenylquinoxaline copolymer systems.[35] In our case, this discrepancy is explained on examination of the thermal history of the sample prior to and in the course of testing. It is likely that samples heated for a period of 3–4 h, to attain a molding temperature of 290°C, had undergone some degradation. This was verified by a DSC study on a solvent-cast film sample which was subjected to a thermal treatment analogous to that of the molded sample. As a result of this treatment, a reduction of ca. 40° was observed in the glass transition temperature. It is therefore thought that the glass transition of the ester lies nearer to 290°C, since this temperature is that obtained without previous heat treatment.

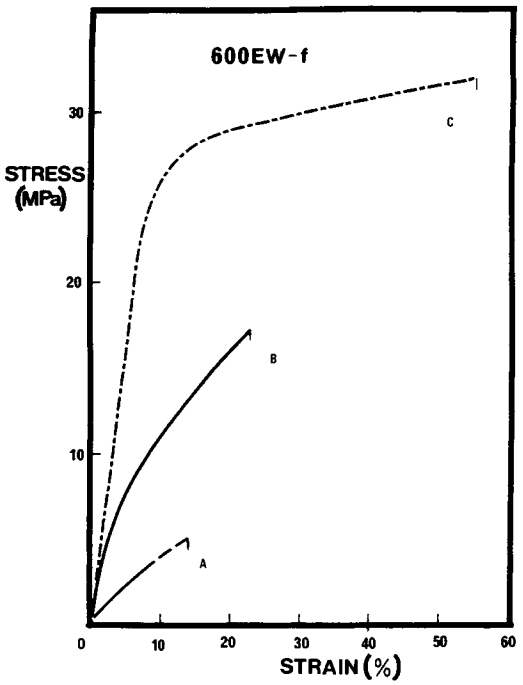

Fig. 11. Stress–strain curves, in 20% potassium hydroxide at 80°C, showing the effect of crosslinking. Elastic modulus values are for: (A) 35 MPa; (B) 150 MPa; (C) 200 MPa.

Differential Scanning Calorimetry

The endotherm which reflects the decarboxylation reaction which marks the onset of degradation at ca. 400°C in the ester precursor material disappears in the fully neutralized ionomers. In those materials which show the presence of residual ester groups, this reaction is shifted to ca. 500°C, and the heat of reaction is much decreased. This is confirmed by TGA, which shows the beginning of weight loss only at 450°C for 600EW-f. Two explanations are possible. The shift of the decarboxylation endotherm to higher temperature may be due to the presence of chemical crosslinks. If we assume that the crosslink consists of a double ester linkage, as shown in eq. (2), then it follows that two bonds instead on one have to be broken for decarboxylation to occur. Alternatively, the shift to higher temperature may be related to a steric effect due to ion incorporation. The decarboxylation reaction may simply be hindered by the increased rigidity of the matrix brought about by Coulombic interaction of the ionic groups.

In this case, consistent with other ionomer systems, the high temperature transitions (Table II) occur at temperatures increasing with increasing ionic content at the rate of 2–3°/mol % ions. It is noteworthy that the specific heat changes associated with these glass transitions uniformly exceed those associated with the transition at 290°C in the first heating experiment only. After quenching, the second heating run still shows a change in heat capacity at 290°C, but the higher temperature glass transition is absent. These facts suggest that a breakdown of ionic associations occurs at the elevated

temperatures reached during the first heating (> 500°C), interactions which do not reform on quenching.

The transition at 290°C which persists in the ionomer samples is puzzling on two counts. Inspection of Figure 3 shows that no corresponding dispersion in the mechanical spectrum is observed at that temperature. Inspection of Table II shows that 290°C is also the glass transition temperature of the ester precursors as determined by DSC. We conclude that this lower temperature transition in the ionomers may be ascribed to motions of these portions of the polymer chains which do not contain ions. As to the torsion pendulum results, it is possible that diffusion occurs during the slow heating which accompanies a run. The diffusion of ionic portions of the polymer may act to minimize the size of these nonionic regions, and this would account for the absence of a loss peak in the 290°C interval.

The multiple distribution of freezing water in 600EW-f samples analyzed by DSC strongly indicates the presence of different structural features in the material. As stated earlier, the results obtained to date are clearly inadequate for a quantitative analysis. A more controlled study is necessary.

Stress–Strain

The stress–strain results on the 600EW ester and ionomer films (Table III) show a decrease of an order of magnitude in the modulus of the ionomer relative to the ester. Clearly, the ionic material is highly plasticized in that aqueous environment. The concentrated alkaline environment does not affect the performance of 600EW-f whereas a decrease in tensile strength and toughness is observed for Nafion 1200 under these conditions. These preliminary results thus confirm the retention of good mechanical properties in 600EW-f under relatively harsh conditions of use.

Strain Orientation

Although the material is essentially amorphous, it can be oriented to an appreciable extent, particularly in the ester form where elongations of ca. 150% are easily obtained. Relatively ordered domains are suggested by wide angle X-ray diffraction of the drawn sample. In the as-cast film, only the amorphous halo is clearly observed. After stretching the sample, complementary diffuse arcs appear in both the equatorial and meridional directions. This indicates an increase in both interchain and single chain orientation.[36]

Contact Angle

The contact angle results shown in Figure 6 are graphic evidence of the wettability of 600EW-f. They suggest that the structure of 600EW-f differs markedly from that of the other films. The continuous decrease in contact angle implies a similar change in the material's surface energy, which could conceivably be due to the presence of ionic groups at the film surface. Porosity is the other structural feature of the aromatic ionomer which cannot be entirely ignored in the interpretation of these preliminary data. The possible inclusion of hydrophilic impurities should also be considered in any treatment of contact angle data in view of deriving surface energies.

High Temperature Limitations

The complex behavior of these materials at high temperature severly limits the methods which can be employed to study such systems. Although TGA results show no weight loss at temperatures below 350°C, both precursors and ionomers clearly undergo some degradation on prolonged exposure to elevated temperatures (i.e., >250°C). The evidence for such degradation comes from DSC, FTIR, and a stress–strain study performed on systematically heat-treated samples. This last study will be treated more extensively in a future publication.

The occurrence of degradation accounts for the inability to draw clear-cut conclusions from such conventional methods as torsion pendulum and high temperature isothermal relaxation techniques. For, although each individual perturbation is of short duration (for, e.g., 1 s, in torsion pendulum), the entire experiment entails keeping the sample at elevated temperatures for several hours. The heating undergone during the molding of the sample must also be taken into consideration. During that time, it is probable that a number of processes occur, possibly including chain scission. Two effects can be envisaged as a direct result of backbone chain scission. One is the plasticization due to an increased number of chain ends. The other is a lowered barrier to diffusion in a medium of decreased molecular weight. Thus, a potentially uneven distribution of ionic groups resulting from the initial polymerization conditions may well shift towards a more homogeneous arrangement. This does not imply chemical bond interchange but rather the breaking and reforming of ionic or electrostatic interactions. Dynamic thermal analysis such as DSC emerges as one of the applicable methods for understanding these systems because the experimental time scale allows observation of molecular processes with only minimal degradation.

CONCLUSION

We have presented some results on a new ionomeric material which differs significantly from those studied to date. The high glass transition temperature is one of the features which sets those systems apart from other ionomers. There is no evidence for ionic cluster formation even at relatively high ionic content. The material retains chemical stability in concentrated alkaline solution, withstands temperatures of up to 290°C, and shows good wettability. These properties, with the exception of wettability, appear to derive more from the relatively rigid aromatic ether backbone than from the incorporation of potassium neutralized carboxylate side groups. However, the salt groups impart to these ionomer films the ability to function in alkaline media as separators which allow ion transport.[37] The presence of these randomly spaced ionic groups is clearly manifested in the calorimetric results, but no conclusive statement can be made as to their organization in the matrix with the data obtained to date.

This work was made possible by the financial support of the National Research Council of Canada. The help of Dr. Martin Hammerli of the NRC is also gratefully acknowledged.

References

1. R. Longworth, in *Developments in Ionic Polymers*, A. D. Wilson and H. J. Prosser Eds., Applied Science Publishers, Barking, UK, 1983, Vol. 1, Chap. 3.
2. C. G. Bazuin and A. Eisenberg, *Ind. Eng. Chem., Prod. Res. Dev.*, **20**, 271 (1981).
3. W. R. Rees and D. J. Vaughan, *Polym. Prepr., Am. Chem. Soc., Div. Polym. Chem.*, **6**, 296 (1965).
4. T. C. Ward and A. V. Tobolsky, *J. Appl. Sci.*, **11**, 2403 (1967).
5. E. P. Otocka and T. K. Kwei, *Macromolecules*, **1**, 301 (1968).
6. E. F. Bonotto, and E. F. Bonner, *Macromolecules*, **1**, 510 (1968).
7. F. C. Wilson, L. Longworth, and D. J. Vaughan, *Polym. Prepr., Am. Chem. Soc., Div. Polym. Chem.*, **9**(1), 505 (1968).
8. K. Sakamoto, W. J. MacKnight, and R. S. Porter, *J. Polym. Sci., Part A-2*, **8**, 277 (1970).
9. S. R. Rafikov, et al., *Vysokomol. Soedin., Ser. A.*, **15**, 1974 (1973).
10. C. L. Marx and S. L. Cooper, *J. Macromol. Sci.*, **B9**, 19 (1974).
11. W. E. Fitzgerald and L. E. Nielsen, *Proc. Roy. Soc. London, Ser. A*, **282**, 137 (1964).
12. N. Z. Erdi and H. J. Morawetz, *J. Colloid Sci.*, **19**, 708 (1964).
13. A. Eisenberg and M. Navratil, *Macromolecules*, **6**, 604 (1973).
14. A. Eisenberg, M. King, and M. Navratil, *Macromolecules*, **6**, 734 (1973).
15. A. Eisenberg and M. Navratil, *Macromolecules*, **7**, 90 (1974).
16. E. Shohamy and A. Eisenberg, *J. Polym. Sci., Polym. Phys. Ed.*, **14**, 1211 (1976).
17. R. D. Lundberg and H. S. Makowski, *Polym. Prepr., Am. Chem. Soc., Div. Polym. Chem.*, **19**(2), 201 (1978).
18. A. Eisenberg and H. L. Yeager, Eds., *Perfluorinated Ionomer Membranes*, ACS Symposium Series 180, Am. Chem. Soc., Washington, D.C., 1982.
19. F. W. Harris et al., Technical Report AFML-TR-76-9, March 1976.
20. F. W. Harris et al., Technical Report AFML-TR-78-98, Wright State University, Dayton, Ohio, July 1978, p. 22.
21. F. W. Harris, B. A. Reinhardt, and R. D. Case, *Polym. Prepr., Am. Chem. Soc., Div. Polym. Chem.*, **19**(2), 394 (1978).
22. M. Rigdahl, A. B. Reinhardt, F. W. Harris, and A. Eisenberg, *Macromolecules*, **14**, 851 (1980).
23. S. Sourirajan, *Reverse Osmosis and Synthetic Membranes*, National Research Council of Canada, Ottawa, 1977.
24. F. D. Snell and C. L. Hilton, Eds., *Encyclopedia of Ind. Chem. Analysis Vol. 1, General Techniques*, Wiley-Interscience, New York, 1966, p. 552.
25. B. Cayrol, Ph.D. Thesis, McGill University, Montreal, 1972.
26. J. Williams, Ph.D. Thesis, McGill University, Montreal, 1978.
27. E. Besso, *J. Appl. Polym. Sci.*, **28**, 1545 (1983).
28. T. Kyu and A. Eisenberg, *J. Polym. Sci., Polymer Symp.* **71**, 203–219 (1984).
29. A. V. Tobolsky, *Properties and Structure of Polymers*, Wiley, New York, 1970.
30. J. D. Ferry, *Viscoelastic Properties of Polymers*, Wiley, New York, 1970.
31. R. Legras, A. Eisenberg, et al., unpublished results.
32. S. Escoubes and M. Pineri, in Ref. 18, Chap. 2.
33. K. Yamada and A. Eisenberg, unpublished.
34. D. J. Pasto and C. R. Johnson, *Organic Structure Determination*, Prentice-Hall, Englewood Cliffs, NJ, 1969, p. 129.
35. P. M. Hergenrother, *Appl. Polym. Symp.*, **22**, 57 (1972).
36. W. O. Statton, *Ann. N.Y. Acad. Sci.*, **83**, 27 (1959).
37. A. Steck and H. L. Yeager, et al., *J. Appl. Polym. Sci.*, to appear.

Received May 7, 1984
Accepted October 22, 1984